

Crystal structures and phase transformations in $\text{Ca}(\text{BH}_4)_2$

Yaroslav Filinchuk^a, Ewa Rönnebro^{b,*}, Dhanesh Chandra^c

^aSwiss-Norwegian Beam Lines at ESRF, BP-220, 38043 Grenoble, France

^bSandia National Laboratories, 7011 East Ave, Livermore, CA 94551-0969, USA

^cUniversity of Nevada, Reno, NV 89557, USA

Received 30 May 2008; received in revised form 10 October 2008; accepted 12 October 2008

Available online 4 December 2008

Abstract

Crystal structures of three polymorphs of $\text{Ca}(\text{BH}_4)_2$, and related phase transitions, have been identified. Removal of solvent from $\text{Ca}(\text{BH}_4)_2 \cdot 2\text{THF}$ results in various mixtures of α - and β -polymorphs of $\text{Ca}(\text{BH}_4)_2$. These mixtures were studied by *in situ* synchrotron powder diffraction in argon atmosphere. The α - $\text{Ca}(\text{BH}_4)_2$ structure crystallizes in the noncentrosymmetric space group $F2dd$, and contains an ordered BH_4^- anion. Upon increasing the temperature, the cell parameters a and c of the α -phase approach each other, and at ~ 495 K, a second order $\alpha \rightarrow \alpha'$ transition takes place resulting in a tetragonal α' -phase of space group $I-42d$, a supergroup of $F2dd$. The structure of β - $\text{Ca}(\text{BH}_4)_2$, which is 3.7–5.6% denser depending on temperature, was described in space group $P-4$. Crystal structures, variation of the cell parameters, and weight fraction are reported for the three $\text{Ca}(\text{BH}_4)_2$ phases as a function of temperature.

© 2008 Acta Materialia Inc. Published by Elsevier Ltd. All rights reserved.

Keywords: In situ synchrotron diffraction; Hydrides; Crystal structure

1. Introduction

With the anticipated “Hydrogen economy”, hydrogen storage is known to be a key enabling method for the advancement of hydrogen and fuel cell power technologies in a variety of applications, including on-board vehicular storage. Many research groups are attempting to find new and practical metal hydrides or other hydrogen storage materials that will meet the US DOE system target of 6 wt.% reversible hydrogen capacity at around 373 K and 1–10 atm [1]. Recently investigated materials with high gravimetric densities include alanates [2], amides [3] and metal borohydrides [4–7]. Among the metal borohydrides, the crystal chemistry of the alkali borohydrides (i.e., LiBH_4 and NaBH_4) is relatively well explored [4–7]. Further, it was shown by Vajo et al. [8] and Bösenberg et al. [9] that by destabilizing LiBH_4 with MgH_2 upon formation of MgB_2 , LiH and hydrogen gas, a system capable of reversibly storing 8–

10 wt.% hydrogen at 623–723 K is obtained. $\text{Mg}(\text{BH}_4)_2$ has also been investigated for its reversible properties [10,11], and was recently shown by Li et al. [12] to be partially reversible to 6.1 wt.% at 400 bar and 270 °C. Another interesting high-hydrogen content compound is $\text{Ca}(\text{BH}_4)_2$, but little information is available regarding its fundamental properties. Calcium borohydride can be prepared by reacting calcium hydride [13] or alkoxides [14] with diborane or by reaction in tetrahydrofuran (THF) [15], to form $\text{Ca}(\text{BH}_4)_2 \cdot 2\text{THF}$, which is commercially available. The solvent can be removed from $\text{Ca}(\text{BH}_4)_2 \cdot 2\text{THF}$ in a vacuum at 463 K [15]. Recently, calcium borohydride was more conveniently prepared by reacting MgB_2 with CaH_2 at 350 bar H_2 -pressure and 673 K, upon obtaining MgH_2 as a by-product [16]. In this reaction the maximum hydrogen capacity of $\text{Ca}(\text{BH}_4)_2$ would be 8.3 wt.%. Nakamori et al. [17] prepared calcium borohydride by ball milling LiBH_4 with CaCl_2 , to obtain LiCl as a by-product, thus preventing reversibility. It was recently demonstrated by Rönnebro and Majzoub [18] how to prepare calcium borohydride by a solid-state reaction route obtaining a product yield of $\sim 60\%$. By reacting CaB_6 with CaH_2 according to: CaB_6 (s) + 2CaH_2

* Corresponding author.

E-mail address: ecronne@sandia.gov (E. Rönnebro).

(s) + 10H₂ (g) → 3Ca(BH₄)₂ (s) a theoretical reversible capacity of 9.6 wt.% hydrogen was anticipated [18]. Further, it was shown that additives are crucial to increase the formation of Ca(BH₄)₂, and it was also noted that different additives result in the formation of different phases. The decomposition products of Ca(BH₄)₂ were predicted to be CaB₆ and CaH₂ by Konoplev and Sizareva [19] and Miwa et al. [20] making this particular reaction formula a good candidate for investigations aimed at reversible H-storage. A recent thermal gravimetry study by Kim et al. [21] indicated partial reversibility also at lower pressures of 90 bar. From laboratory powder X-ray diffraction the structure of high-pressure synthesized calcium borohydride was proposed to be of Ba(MnO₄)₂-type, space group *Fddd* (No. 70) [18] in accordance with the theoretical predictions by Vajeeston et al. [22] and the Rietveld analysis of experimental data by Miwa et al. [20] of an adduct-free sample of calcium borohydride. Recently, Majzoub and Rönnebro [23] identified four low energy crystal structures for Ca(BH₄)₂, predicted by the method of prototype electrostatic ground states (PEGS) [24]. All of them have likely been observed in several X-ray diffraction experiments, our own and others [18,20,25]. To gain a more detailed understanding of the stability and temperature dependence of the polymorphs during thermal desorption of calcium borohydride, we report here on high-quality *in situ* synchrotron diffraction studies of Ca(BH₄)₂, which reveal new crystal structures and phase transformations.

2. Methods

2.1. Synthesis

Miwa et al. [20] reported that an almost pure sample of Ca(BH₄)₂ can be prepared by heating up a sample of Aldrich's Ca(BH₄)₂·2THF in a vacuum at 433 K for 1 h. We tried to repeat this procedure, but we were not successful in obtaining a single-phase sample. After several attempts to prepare Ca(BH₄)₂ by heating Aldrich's Ca(BH₄)₂·2THF at different temperatures in a vacuum, we were able to prepare a sample containing Ca(BH₄)₂ with a similar XRD-pattern to the one reported by Miwa et al. [20], but also containing a second phase which we will discuss in detail below. We loaded 1–2 g samples into stainless steel sample holders and installed them into a rough pump system for initial reaction. All sample handling was executed in an argon filled glove box monitored to have oxygen and water levels below 3 ppm. The temperature was stabilized between 423–428 K for 2 to 3 days. We then installed the sample reactor onto a turbo-pumped residual gas analyzer (RGA) system and monitored gas peaks as well as the pressure at 423 K. We continued heating up the sample under vacuum until the base pressure was achieved, and the level of organic molecules reached a minimum after several days. The sample was analyzed by an in-house powder diffractometer to verify phase compositions. X-ray diffraction is however not conclusive regarding analysis of very small amounts of remaining THF, thus we performed complimentary differential

scanning analysis (DSC) utilizing a Mettler Toledo instrument DSC822 to confirm that the product was free from solvent by observing phase transitions. Thermal analysis of Aldrich's Ca(BH₄)₂·2THF show unique features correlated to release from THF breakdown between 423 and 428 K, thus, we were able to confirm a solvent free product. The sample was thereafter analyzed by an using an *in situ* analytical X-ray diffraction system equipped with XRK 900 Anton Paar (hydrogen) stage at University of Nevada, Reno, where the phase transitions in Ca(BH₄)₂ were first observed.

2.2. Synchrotron powder diffraction study

The fully unsolvated product consists mostly of α -Ca(BH₄)₂ but also some amount of another phase, which we hereafter refer to as the β -phase for reasons that will become obvious. This sample contains 87% α -phase + 13% β -phase, as quantified from the below described Rietveld refinements, and was studied by *in situ* synchrotron powder diffraction. The sample was placed in a (0.5 mm diameter) glass capillary and sealed under argon. Thereafter, heated from 80 to 500 K at a rate of 60 K/h while synchrotron powder diffraction data were collected. Temperature was controlled with an Oxford Cryostream 700+.

Moreover, additional studies were conducted at elevated temperatures (317–573 K) at a heating rate of 120 K/h. The sample was heated to 573 K and held for 2 h while we measured the diffraction data. The sample was then cooled to 305 K, and thereafter, a second heating cycle was performed from 305 to 873 K at a rate of 120 K/h. A Cyberstar ESRF furnace and a Eurotherm temperature controller were used for these experiments.

Diffraction data were collected using an MAR345 image plate detector at the BM01A line of SNBL (ESRF). The data were measured at a sample to detector distance of 150 mm (the above mentioned additional studies were conducted at 200 mm), using radiation of $\lambda = 0.711385$ Å. The capillaries were oscillated by 60° during exposure to the X-ray beam for 60 s, followed by a readout for ~83 s. In total, 518 diffraction images were collected (326 at 80–500 K, 82 at 317–573 K and 110 at 305–873 K). The hump on the background at ~10° corresponds to scattering of X-rays on the glass capillary (amorphous). This low-frequency wave has been easily modelled in presence of sharp diffraction peaks from the crystalline sample.

The data were integrated using the Fit2D program [26]. We performed an external calibration using the NIST LaB₆ standard sample. Uncertainties of the integrated intensities $\sigma(I)$ were calculated at each 2θ -point by applying Poisson statistics to the intensity data, considering the geometry of the detector. The procedure of $\sigma(I)$ estimation is identical to the one used by Vogel et al. [27]. A common disadvantage of having relatively weak diffraction intensities at high 2θ was compensated for by large counting statistics, exceeding in 10⁷ counts per step in 2θ . Properly weighted, these intensities contributed to the accurate determination of the crystal structures.

3. Results and discussion

3.1. Determination of crystal structures of $\text{Ca}(\text{BH}_4)_2$ polymorphs

A detailed analysis of the *in situ* diffraction data was performed and will hereafter be described with focus on the α -, α' - and β -phases in consecutive order. Another *in situ* synchrotron experiment was recently performed by Riktor et al. [25], presenting polymorphs labeled as β , γ , and δ , but no crystal structures were reported. Their β -phase is likely the same as the one we present here, but we don't observe the γ and δ phases. The structure of the α -phase was solved *ab initio* using a global optimization program FOX [28]. The structure was refined by the Rietveld method with FullProf [29]. Four space groups were tested: *Fddd*, *F2dd*, *Fd2d* and *Fdd2*, using the orthorhombic $8.78 \times 13.02 \times 7.41 \text{ \AA}$ cell. Best fit was obtained with the *F2dd* and *Fdd2* space groups. It is not possible to conclude from systematic extinctions which of the two glide planes have to be removed. However, in our refinements, the *F2dd* structure provided a better fit (χ^2 lower by 5–10%) than the *Fdd2* model throughout all the data series (see Section 3.3). Moreover, the shortest H...H distance between two BH_4 anions in the refined *F2dd* model are longer ($\sim 2.34 \text{ \AA}$), than for the *Fdd2* model ($\sim 2.29 \text{ \AA}$), and even longer than in the refined *Fddd* model (2.07 \AA). The structure of α - $\text{Ca}(\text{BH}_4)_2$ was described from laboratory XRD of a solvent free adduct of $\text{Ca}(\text{BH}_4)_2 \cdot 2\text{THF}$ (prepared in the same way as our sample) to have a structure described in *Fddd* as reported by Miwa et al. [20], but here, from high-quality synchrotron data, we found another space group. Refinement of our data in the *Fddd* model [20] did not result in a satisfying fit. The obtained criteria of fit were: $R_B = 19.3\%$, $R_F = 9.0\%$, $R_p = 5.5\%$, and $R_{wp} = 7.0\%$ (not corrected for background), $R_p = 23.1\%$, and $R_{wp} = 23.6\%$ (conventional Rietveld *R*-factors). Thus,

the calculated pattern did not fit well with the observed one. The *F2dd* structure was refined using 279 reflections, 27 intensity-dependent refined parameters, and 10 soft restraints defining an approximately tetrahedral BH_4 geometry. It is important to note that our unrestrained refinement of BH_4 in the *F2dd* symmetry anion yielded a nearly ideal tetrahedral geometry, compared to a distorted geometry for the *Fddd* model. The background was modelled by interpolated points. The refinement converged at $R_B = 3.3\%$, $R_F = 3.0\%$, $R_p = 1.5\%$, and $R_{wp} = 2.1\%$ (not corrected for background), $R_p = 5.9\%$, and $R_{wp} = 7.0\%$ (conventional Rietveld *R*-factors). Atomic and cell parameters are listed in Table 1, and the fit to the experimental data is shown in Fig. 1a. Fig. 1b shows the difference plot from the refinements in space group *Fddd*, clearly showing the non-satisfying fit. It is important to note that elimination of hydrogen atoms for the α -phase increases R_B from 3.0% to 9.1%.

When the sample is heated up to higher temperatures, another structural arrangement of $\text{Ca}(\text{BH}_4)_2$ was observed. Upon heating, the α -phase cell parameter *a* is observed to increase, whereas the *c* parameter decreases until it finally transforms to the tetragonal α' -phase at 495 K. The continuous approach of the lattice parameters implies a second order transition, and so the α' -phase can take only one of the three minimal supergroups of *F2dd*: *I4₁md*, *I4₁cd* and *I-42d*. The *I4₁cd* is not compatible with observed systematic extinctions, and was therefore rejected as a solution. Structure solution was attempted in the remaining two space groups using FOX [28]. The structure was solved in *I-42d* and refined with Fullprof against the data collected at 495 K using 68 reflections, 10 intensity-dependent refined parameters, and 6 soft restraints to define an approximately tetrahedral BH_4 geometry. The BH_4 anion refined without restraints shows a nearly ideal tetrahedral geometry. The background was modelled by interpolated points. The refinement converged at $R_B = 5.4\%$, $R_F = 7.1\%$,

Table 1
Experimental structural parameters for the $\text{Ca}(\text{BH}_4)_2$ polymorphs obtained from synchrotron powder diffraction data.

| Structure | Atom | x | y | z | B (\AA^2) |
|---|------------|-------------|-------------|-------------|----------------------|
| α -phase at 91 K <i>F2dd</i> , <i>Z</i> = 8 <i>a</i> = 8.7759(3) <i>b</i> = 13.0234(4) <i>c</i> = 7.4132(2) \AA | Ca | 0 | 0 | 0 | 1.53(3) |
| | B | 0.0056(9) | 0.2243(2) | 0.0081(11) | 1.60(8) |
| | H1 | 0.0190(19) | 0.1648(10) | 0.1272(16) | 0.2(3) |
| | H2 | 0.0345(19) | 0.1817(11) | −0.1256(14) | 0.2(3) |
| | H3 | −0.1180(10) | 0.2553(12) | 0.012(2) | 0.2(3) |
| H4 | 0.0910(15) | 0.2922(9) | 0.028(2) | 0.2(3) | |
| α' -phase at 495 K <i>I-42d</i> , <i>Z</i> = 4 <i>a</i> = 5.8446(3) <i>c</i> = 13.2279(11) \AA | Ca | 0 | 0 | 0 | 5.67(16) |
| | B | 0 | 0 | 0.2250(6) | 4.3(3) |
| | H1 | −0.1608(16) | −0.035(3) | 0.1762(10) | 0(1) |
| | H2 | 0.032(3) | −0.1613(16) | 0.2752(10) | 0(1) |
| β -phase at 305 K <i>P-4</i> , <i>Z</i> = 2 <i>a</i> = 6.91894(11) <i>c</i> = 4.34711(12) \AA | Ca | 0.5 | 0 | 0.240(2) | 3.37(4) |
| | B | 0.790(1) | 0.693(9) | 0.259(2) | 4.26(14) |
| | H1 | 0.626(2) | 0.727(2) | 0.217(5) | 6.0(9) |
| | H2 | 0.833(3) | 0.765(2) | 0.491(3) | 6.0(9) |
| | H3 | 0.808(3) | 0.528(1) | 0.262(5) | 6.0(9) |
| | H4 | 0.873(3) | 0.769(1) | 0.062(5) | 6.0(9) |

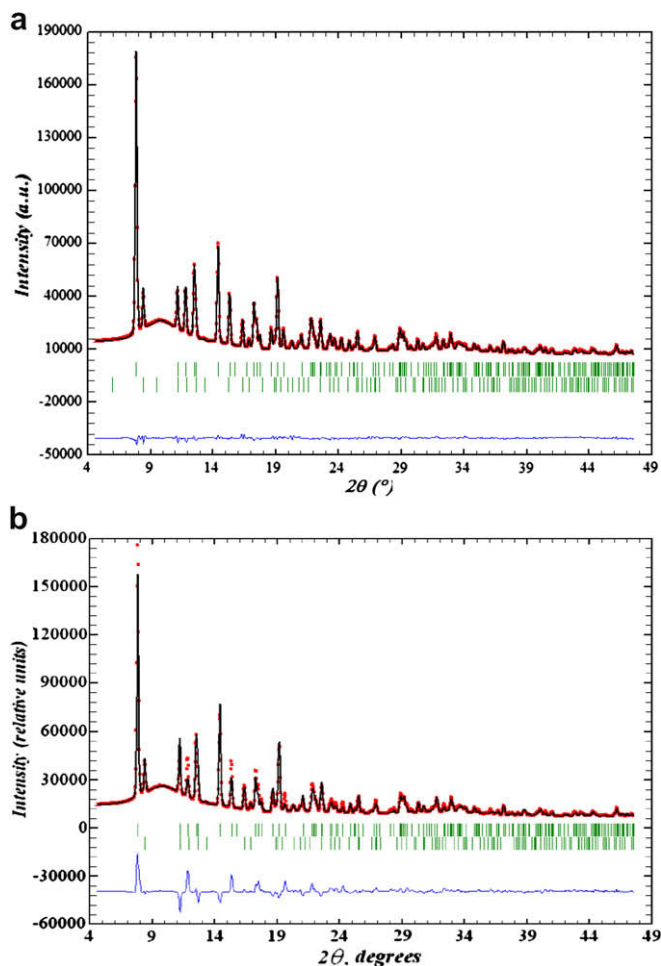


Fig. 1. (a) Rietveld refinement profile at 91 K, containing $\sim 87\%$ of the α - $\text{Ca}(\text{BH}_4)_2$ and $\sim 13\%$ of the β - $\text{Ca}(\text{BH}_4)_2$ modelled in the space groups $F2dd$ and $P-4$, respectively. (b) Rietveld refinement profile (same data set as in (a)) showing α - $\text{Ca}(\text{BH}_4)_2$ modelled in space group $Fddd$.

$R_p = 1.0\%$, and $R_{wp} = 1.5\%$ (not corrected for background), $R_p = 10.7\%$, and $R_{wp} = 10.3\%$ (conventional Rietveld R -factors). Atomic and cell parameters are listed in Table 1, and the fit to the experimental data is shown in Fig. 2. Again, it is important to note that elimination of hydrogen atoms increases R_B from 5.4% to 12.0%.

Finally, we will focus on the crystal structure of β - $\text{Ca}(\text{BH}_4)_2$ which was observed in the phase mixture of α - and β -phases, as obtained by removal of solvent (as described in Section 2.1). The powder diffraction pattern, collected at 305 K, contained only a small amount of weak impurity peaks of the decomposition products. Therefore, the dataset was indexed by DICVOL2004 [30] in a primitive tetragonal cell ($a = 6.92$, $c = 4.35$ Å). Its structure was originally solved by using the program FOX [28] starting from Ca atoms and rigid BH_4 tetrahedra as building blocks, in space group $P4_2nm$ (No. 102). However, the refined structure contains slightly too short Ca–H distances of 1.87 Å. Majzoub and Rönnebro [23] recently determined the β -polymorph to be best described in space group $P-4$ (No. 81) or $P4_2/m$ (No. 84) by a combined theoretical

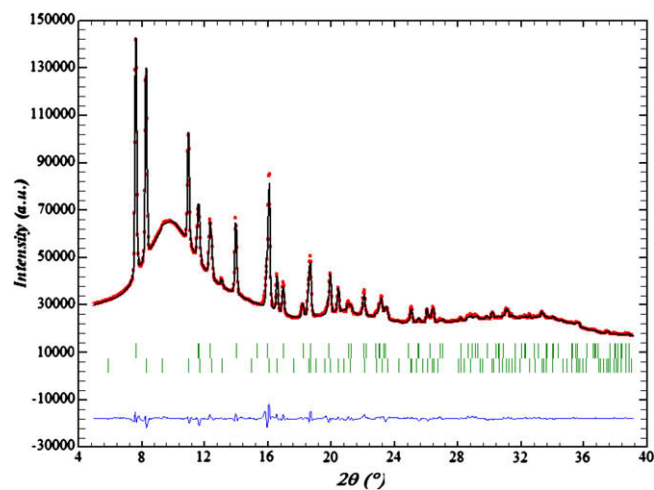


Fig. 2. Rietveld refinement profile for the α' - $\text{Ca}(\text{BH}_4)_2$ (space group $I-42d$) at 495 K, $\lambda = 0.711385$ Å. $\sim 50\%$ of the β - $\text{Ca}(\text{BH}_4)_2$ has been modelled in the space group $P-4$.

and experimental approach, using the PEGS (Prototype Electrostatic Ground State) method to find lowest energy structures. The Rietveld refinements indicated that the structure could preferably be described in $P-4$. This structure model of the β -phase was verified here on a single-phase sample, obtained by annealing the $\alpha + \beta$ mixture at 573 K. At this temperature, the conversion from the α to β -phase has been completed. The $P-4$ model showed slightly better fit than the $P4_2nm$ one, but more importantly, more reasonable interatomic distances. Thus, finally the $P-4$ structure was refined by the Rietveld method with FullProf. We used 64 reflections, 12 intensity-dependent refined parameters, and 10 soft restraints defining an approximately tetrahedral BH_4 geometry. During the refinement, the background was modelled by interpolated points. The refinement converged at $R_B = 4.2\%$, $R_F = 5.1\%$, $R_p = 1.0\%$, and $R_{wp} = 1.4\%$ (not corrected for background), $R_p = 9.8\%$, and $R_{wp} = 7.2\%$ (conven-

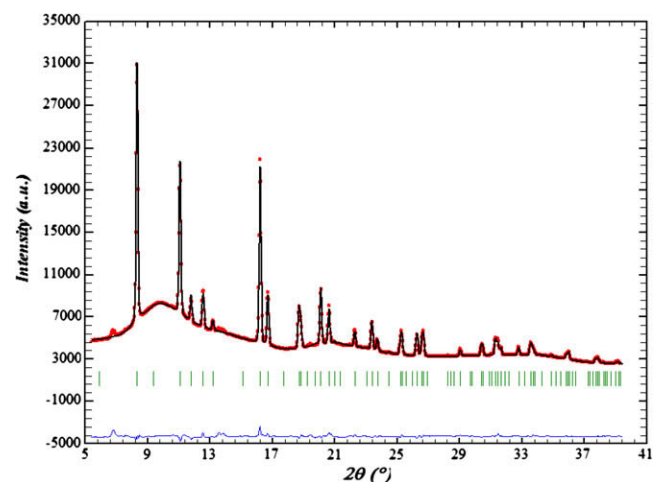


Fig. 3. Rietveld refinement profile for the β - $\text{Ca}(\text{BH}_4)_2$ (space group $P-4$) at 305 K, $\lambda = 0.711385$ Å. Weak impurity peaks correspond to decomposition products.

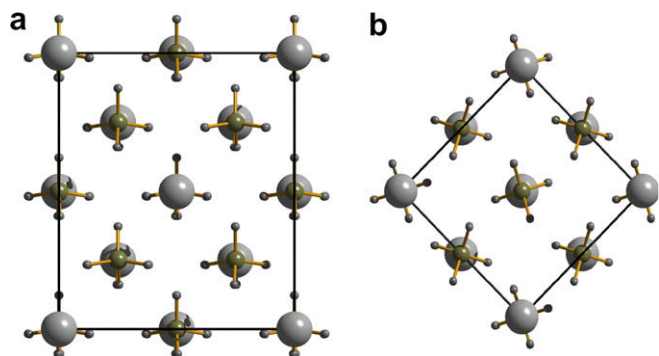


Fig. 4. Projections of the α and α' - $\text{Ca}(\text{BH}_4)_2$ structures, refined using our experimental data. Ca atoms shown as big spheres. (a) α - $\text{Ca}(\text{BH}_4)_2$ ($F2dd$) projected on the ac plane. (b) α' - $\text{Ca}(\text{BH}_4)_2$ ($I-42d$) projected on the ab plane.

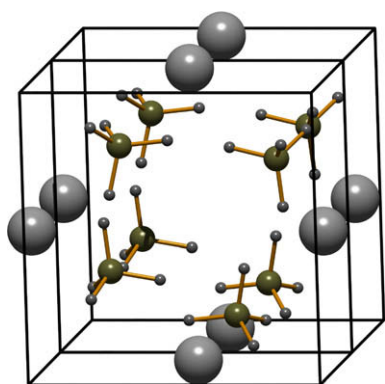


Fig. 5. Crystal structure of the β - $\text{Ca}(\text{BH}_4)_2$, space group $P-4$. Ca atoms shown as big spheres.

tional Rietveld R -factors). Atomic and cell parameters are listed in Table 1, and the fit to the experimental data is shown in Fig. 3. It is worth noting that elimination of hydrogen atoms increases R_B from 4.2% to 9.4%, thus showing that their contribution to X-ray diffraction intensities is sufficient for localization of H-atoms, even from powder diffraction data [4–6]. Buchter et al. [31] chose to describe the β -structure in $P4_2/m$ based on neutron diffraction and synchrotron data of a sample containing seven different phases, however, our refinements in $P4_2/m$ resulted in higher R -values: $R_B = 5.19\%$, $R_F = 5.46\%$, $R_p = 1.2\%$, and $R_{wp} = 1.5\%$ (not corrected for background), $R_p = 10.9\%$, and $R_{wp} = 8.1\%$ (conventional Rietveld R -factors).

3.2. Crystal chemistry

The crystal structures of $\text{Ca}(\text{BH}_4)_2$ contain calcium cations nearly octahedrally coordinated by six borohydride anions. Coordination numbers for the alkaline-earth atoms correlate with their radii, and change from 3 in $\text{Be}(\text{BH}_4)_2$ [32] to 4 in $\text{Mg}(\text{BH}_4)_2$ [33,34], and finally to 6 in the three $\text{Ca}(\text{BH}_4)_2$ structures. Although the $\text{Ca}(\text{BH}_4)_2$ structures described here were determined at different temperatures,

they show directly comparable interatomic distances. Thus, the six Ca–B distances in each of the experimentally determined structures are within similar narrow ranges of 2.816(8)–2.967(8) Å for the α -phase at 91 K, 2.941(1)–2.976(8) Å for the α' -phase at 495 K and 2.923(8)–2.939(8) Å for the β -phase at 305 K. Essential interatomic distances and angles involving hydrogen atoms in all the three polymorphs are listed in Table 2.

Ca atoms form a T-shaped arrangement around the B atoms in the α - and α' -phases and a nearly triangular arrangement in the β -phase (Ca...B...Ca angles 95.5–133.7°). Correspondingly, the coordination mode for the BH_4^- anion with respect to the Ca cations also differs. In the closely related structures of the α - and α' -phases (Fig. 4), the orientation of the BH_4^- tetrahedron is such that it bridges three Ca^{2+} ions via the tetrahedral edges. In the α -phase the Ca...H₂B coordination is somewhat asymmetric with Ca–H distances of 2.23–2.81 Å. In the α' -phase each Ca atom coordinates two BH_4 groups via the edge (Ca...H₂B, with Ca–H distances 2.52 Å), and other four via the corner (Ca...HB, with Ca–H distances 2.02 Å). Coordination via the edge is typical for alkaline [4–7] and alkaline-earth borohydrides, such as $\text{Be}(\text{BH}_4)_2$ [32] and $\text{Mg}(\text{BH}_4)_2$ [33,34]. In the β -phase (Fig. 5), similarly to the α' -phase, two Ca atoms coordinate the BH_4 groups via edges, and the third one via a tetrahedral vertex. The experimentally determined Ca–H distances vary from 2.08 to 2.56 Å. A possibility to refine the structure of the β -phase in various tetragonal space groups, where the orientation of the BH_4 group slightly differs, suggests a possible uncertainty of the BH_4 localization and thus may indicate that the β -phase is stabilized by static or dynamic disorder of the borohydride group, similar to the high-temperature phase of LiBH_4 [35]. To verify this, a neutron diffraction experiment on isotopically labeled $\text{Ca}^{11}\text{BD}_4)_2$ would be appropriate. Buchter et al. [31] recently reported neutron diffraction data from a multiphase sample containing $\text{Ca}^{11}\text{BD}_4)_2$ and MgD_2 , prepared by ball milling MgB_2 plus CaD_2 , reaching a similar conclusion regarding the crystal structures of the β -phase as presented here. However, we have chosen a different space group based on our theoretical [23] and single-phase experimental data and obtaining a slightly better fit when describing the structure in $P-4$ instead of $P4_2/m$. It is important to consider that it is possible that different synthesis routes of $\text{Ca}(\text{BH}_4)_2$ can result in different degree of order of the BH_4 unit. The crystal structure of a mechanically alloyed sample, such as prepared by Buchter et al. [31], is likely more disordered, as indicated by the amorphous-like NPD-pattern in their paper, compared to the sample prepared here by removing the solvent and resulting in a highly crystalline product.

The refined geometry of the BH_4^- anions was restrained to an ideal tetrahedral configuration with the B–H bond length centered at ~ 1.17 Å. The fit to the diffraction data showed that these assumptions are consistent with the experimental data. The assumed B–H distance is close to the average B–H distance of 1.12 Å known from single

Table 2

Essential interatomic distances (Å) and angles (°) in the three Ca(BH₄)₂ polymorphs studied by synchrotron powder diffraction.

| Phase | B–H | H–B–H | H...H within BH ₄ | min. H...H between BH ₄ | Ca–H |
|---------------------------------|-----------------|-----------------|------------------------------|------------------------------------|-----------------|
| α : 91 K, <i>F2dd</i> | 1.16(1)–1.18(1) | 108(1)–113(1) | 1.85(2)–1.94(2) | 2.34(2) | 2.23(1)–2.81(2) |
| α' : 495 K, <i>I-42d</i> | 1.16(1)–1.17(1) | 108(1)–112.3(7) | 1.88(2)–1.92(1) | 2.25(2) | 2.02(2)–2.52(2) |
| β : 305 K, <i>P-4</i> | 1.15(6)–1.17(2) | 106(1)–114(1) | 1.86(3)–1.93(2) | 2.41(3) | 2.08(1)–2.56(2) |

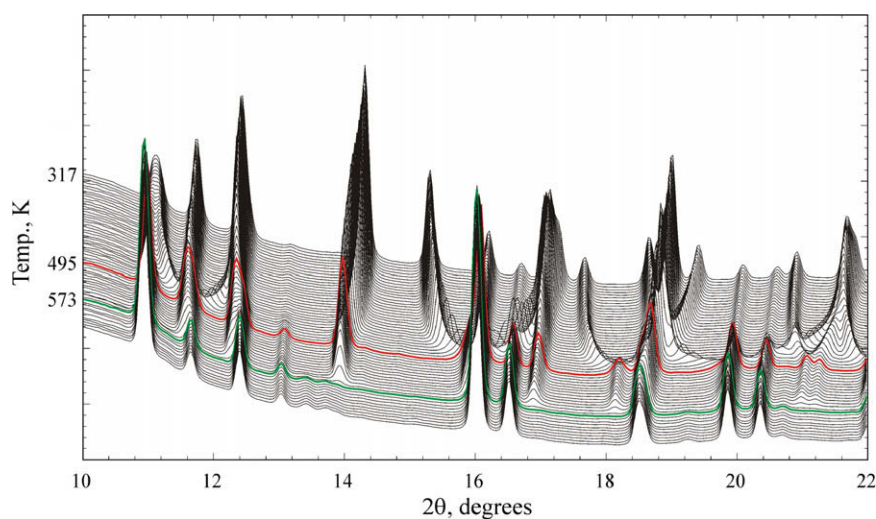


Fig. 6. *In situ* synchrotron powder diffraction data collected at 317–573 K, $\lambda = 0.711385$ Å. Completion of the α - to α' and α' - to β -transitions is highlighted in red and green, respectively. (For interpretation of color mentioned in this figure the reader is referred to the web version of the article.)

crystal X-ray diffraction data on a light metal hydride [35,36]. The shortest H...H distances are 2.34 Å in the α -phase, 2.25 Å in the α' -phase, and 2.41 Å in the structure of the β -phase.

Long Ca...Ca distances (4.3415(1) Å in the α -phase, 4.3471(1) Å in the β -phase, 4.4132(2) Å in the α' -phase) indicate a repulsive interaction. There is, however, an important difference in arrangement of Ca atoms: in the α - and α' -phases the shortest Ca...Ca contacts form a diamond-like substructure, while in the β -phase they form linear chains.

In agreement with the second order of the α - to α' -transition, the α' -phase reveals the *I-42d* symmetry, which is the minimal order supergroup of *F2dd*. An attempt to solve the structure of the α' -phase in the space group *I4₁/amd* (supergroup of *Fddd*) led to a disordered structure, compared to the fully ordered structure in *I-42d*.

Determination of the α -Ca(BH₄)₂ structure and discovery of the new Ca(BH₄)₂ phases with different structures call for calculation of the heat of formation of Ca(BH₄)₂ in order to verify the proposed linear correlation between the Pauling electronegativity of the cation and the heat of formation of metal borohydrides [20].

3.3. Temperature-induced phase transitions

In situ diffraction data, collected within the 317–573 K range are shown in Fig. 6. All three calcium borohydride phases are observed in this region. The unit cell parameters are presented as a function of temperature in Fig. 7. Temperature dependence of the *a* and *c* parameters (see

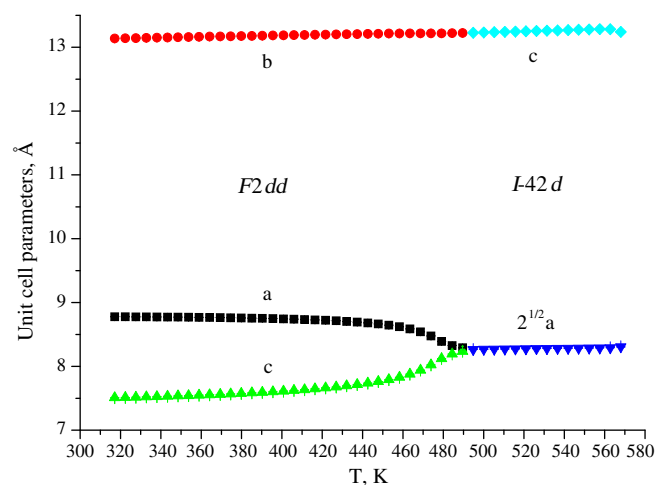


Fig. 7. Variation of the unit cell parameters of the α and α' -Ca(BH₄)₂ as a function of temperature.

Fig. 7) reveals a second order transition from the *F2dd* to *I-42d* phase. The volume of the Ca(BH₄)₂ formulae unit is plotted as a function of temperature in Fig. 8. The β -phase is 3.7–5.6% denser than the α - and α' -phases, depending on the temperature, the latter polymorphs transform into the stable β -phase in the temperature range of 450–570 K. From 305 K and up to decomposition, the unit cell parameters *a* and *c* (Å) and the unit cell volume (Å³) of the β -Ca(BH₄)₂ increase linearly with temperature (K): $a = 6.9187(1) + 2.821(7) \times 10^{-4} T$, $c = 4.34459(9) + 2.062(5) \times 10^{-4} T$, $V = 207.938(5) + 2.725(3) \times 10^{-2} T$. Further, β -Ca(BH₄)₂ completely decomposes between

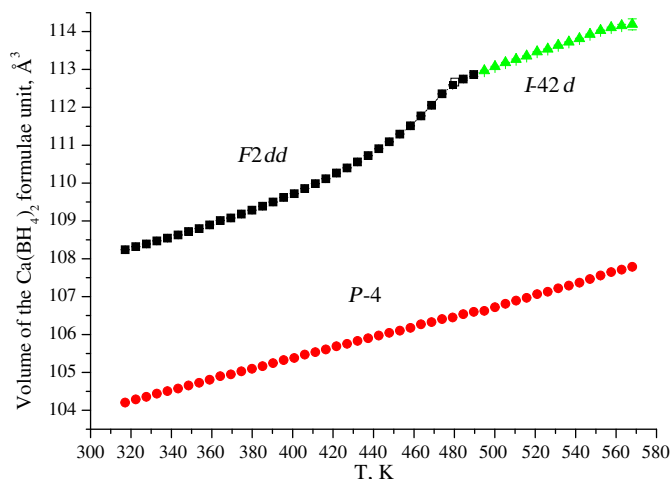


Fig. 8. Volume of the $\text{Ca}(\text{BH}_4)_2$ formulae unit in the α ($F2dd$), α' ($I-42d$) and β -polymorphs ($P-4$) as a function of temperature.

655 and 660 K. Some new crystalline phase(s) appear at higher temperatures, but further investigation is needed to confirm composition. A recent paper by Fichtner et al. [37] described vibrational spectra of $\text{Ca}(\text{BH}_4)_2$, obtained from α -, β -, and γ -phases. During heating, they did not observe the transition of the α -phase to the α' -phase, but, instead, directly to the β -phase.

The weight fraction of the $P-4$ phase shows complex behavior during constant rate heating. At temperatures below 453 K, the content of the $P-4$ phase stays constant. Above 453 K it starts to grow quickly, but after the $F2dd$ to $I-42d$ transition at ~ 493 K, the growth slows down. Finally, at 551 K, the fraction of the $P-4$ phase grows quickly until a full conversion is achieved at ~ 573 K. Thus, the $F2dd$ to $I-42d$ transition and a conversion from $F2dd$ and $I-42d$ phases to the $P-4$ one may be somehow related.

4. Conclusion

In situ synchrotron data collected in argon revealed the crystal structures of two polymorphs of $\text{Ca}(\text{BH}_4)_2$, labeled α -phase ($F2dd$) and β -phase ($P-4$), formed upon removal of solvent from $\text{Ca}(\text{BH}_4)_2 \cdot 2\text{THF}$, and a third polymorph, α' -phase ($I-42d$), formed upon a second order transformation of the α -phase at 495 K. The α - and β -phases were described in different space groups than previously reported in the literature. The α' -phase changes into the β -phase upon heating above 453 K and decomposes at 655 K into unknown products.

Acknowledgments

Funding was partially provided by the US Department of Energy, Office of Energy Efficiency and Renewable Energy under the Hydrogen Storage Grand Challenge, and the Metal Hydride Center of Excellence within DOE's National Hydrogen Storage Project. We thank Ken Stewart at SNL for skillful technical assistance. YF is grateful to

SNBL for the provision of the in-house beam time. Lennie Klebanoff is acknowledged for valuable comments and discussions.

References

- [1] US Department of Energy Hydrogen Program. Available from: <http://www.hydrogen.energy.gov>.
- [2] Bogdanovic B, Schwickardi M. *J Alloys Compd* 2002;339:299.
- [3] Chen P, Xiong X, Lou J, Lin J, Tan KL. *Nature* 2002;420:302.
- [4] Filinchuk Y, Chernyshov D, Nevidomskyy A, Dmitriev V. *Angew Chem Int Ed* 2008;47:529.
- [5] Dmitriev V, Filinchuk Y, Chernyshov D, Talyzin AV, Dzwilewski A, Andersson O, et al. *Phys Rev B* 2008;77:174112.
- [6] Filinchuk Y, Talyzin AV, Chernyshov D, Dmitriev V. *Phys Rev B* 2007;76:092104.
- [7] Filinchuk Y, Hagemann H. *Eur J Inorg Chem* 2008;3127.
- [8] Vajo JJ, Skeith SL, Mertens FJ. *J Phys Chem B* 2005;109:3719.
- [9] Bösenberg U, Doppiu S, Mosgaard L, Barkhordarian G, Eigena N, Borgschulte A, et al. *Acta Mater* 2007;55:3951.
- [10] Chlopek K, Frommen C, Léon A, Zabara O, Fichtner M. *J Mater Chem* 2007;17:3496.
- [11] Zhao JC, Andrus M, Cui J, Gao Y, Kniajansky S, Lemmon J et al. DOE Annual merit review proceedings, hydrogen storage program, metal hydride center of excellence; 2007. Available from: http://www.hydrogen.energy.gov/pdfs/review07/st_16_zhao.pdf.
- [12] Li HW, Kickuchi K, Nakamori Y, Miwa K, Towata S, Orimo S. *Acta Mater* 2008;56:1342.
- [13] Wiberg E, Hartwimmer RZ. *Z Naturforsch* 1955;10b:295.
- [14] Wiberg E, Noth H, Hartwimmer RZ. *Z Naturforsch* 1955;10b:292.
- [15] Mikheeva VI, Titov LV. *Zh Neorg Khim* 1964;9:789.
- [16] Barkhordarian G, Klassen T, Dornheima M, Bormann R. *J Alloys Compd* 2007;440:L18.
- [17] Nakamori Y, Li HW, Kikuchi K, Aoki M, Miwa K, Towata S, et al. *J Alloys Compd* 2007;446–447:296.
- [18] Rönnebro E, Majzoub EH. *J Phys Chem B* 2007;111:12045.
- [19] Konoplev VN, Sizareva AS. *Koord Khim* 1952;18:508.
- [20] Miwa K, Aoki K, Noritake T, Ohba N, Nakamori Y, Towata S, et al. *Phys Rev B* 2006;74:155122.
- [21] Kim JH, Jin SA, Shim JH, Cho YW. *Scripta Mater* 2008;58:481.
- [22] Vajeeston P, Ravindran P, Fjellvåg H. *J Alloys Compd* 2007;446–447:44.
- [23] Majzoub EH, Rönnebro E, submitted for publication..
- [24] Majzoub EH, Ozolins V. *Phys Rev B* 2008;77:104115.
- [25] Riktor MD, Sorby MH, Chlopek K, Fichtner M, Buchter F, Züttel A, et al. *J Mater Chem* 2007;17:4939.
- [26] Hammersley AP, Svensson SO, Hanfland M, Fitch AN, Häusermann D. *High Pressure Res* 1996;14:235.
- [27] Vogel S, Ehm L, Knorr K, Braun G. *Adv X-ray Anal* 2002;45:31.
- [28] Favre-Nicolin V, Cerný R. *J Appl Cryst* 2002;35:734.
- [29] Rodriguez-Carvajal J, FULLPROF SUITE: LLB Sacleay & LCSIM Rennes, France; 2003.
- [30] Boulitif A, Louër D. *J Appl Crystallogr* 2004;37:724.
- [31] Buchter F, Lodziana Z, Remhof A, Friedrichs O, Borgschulte A, Mauron P, et al. *J Phys Chem B* 2008;112:8042.
- [32] Marynick DS, Lipscomb WN. *Inorg Chem* 1972;11:820.
- [33] Cerný R, Filinchuk Y, Hagemann H, Yvon K. *Angew Chem Int Ed* 2007;46:5765.
- [34] Her JH, Stephens PW, Gao Y, Soloveichik G, Rijssenbeek J, Andrus M, et al. *Acta Cryst B* 2007;63:561.
- [35] Filinchuk Y, Chernyshov D, Cerný R. *J Phys Chem C* 2008;112:10579.
- [36] Filinchuk YE, Yvon K, Meisner GP, Pinkerton FE, Balogh MP. *Inorg Chem* 2006;45:1433.
- [37] Fichtner M, Chlopek K, Longhini M, Hagemann H. *J Phys Chem C* 2008;112:11575.